



UNIVERSITY OF LEEDS

This is a repository copy of *Enhancement of bauxite residue as a low-cost adsorbent for phosphorus in aqueous solution, using seawater and gypsum treatments*.

White Rose Research Online URL for this paper:
<http://eprints.whiterose.ac.uk/126267/>

Version: Accepted Version

Article:

Cusack, PB, Healy, MG, Ryan, PC et al. (4 more authors) (2018) Enhancement of bauxite residue as a low-cost adsorbent for phosphorus in aqueous solution, using seawater and gypsum treatments. *Journal of Cleaner Production*, 179. pp. 217-224. ISSN 0959-6526

<https://doi.org/10.1016/j.jclepro.2018.01.092>

(c) 2018 Elsevier Ltd. Licensed under the Creative Commons Attribution-Non Commercial No Derivatives 4.0 International License (<https://creativecommons.org/licenses/by-nc-nd/4.0/>).

Reuse

This article is distributed under the terms of the Creative Commons Attribution-NonCommercial-NoDerivs (CC BY-NC-ND) licence. This licence only allows you to download this work and share it with others as long as you credit the authors, but you can't change the article in any way or use it commercially. More information and the full terms of the licence here: <https://creativecommons.org/licenses/>

Takedown

If you consider content in White Rose Research Online to be in breach of UK law, please notify us by emailing eprints@whiterose.ac.uk including the URL of the record and the reason for the withdrawal request.



eprints@whiterose.ac.uk
<https://eprints.whiterose.ac.uk/>

1 Enhancement of bauxite residue as a low-cost adsorbent for phosphorus in aqueous solution,
2 using seawater and gypsum treatments.

3

4 Patricia B. Cusack^{a,b,c}, Mark G. Healy^{b*}, Paraic C. Ryan^b, Ian T. Burke^d, Lisa M. T. O'
5 Donoghue^e, Éva Ujaczki^{c,e,f}, Ronan Courtney^{a,c}

6

7 ^aDepartment of Biological Sciences, University of Limerick, Castletroy, Co. Limerick, Ireland.

8 ^bCivil Engineering, National University of Ireland, Galway, Ireland.

9 ^cThe Bernal Institute, University of Limerick, Castletroy, Co. Limerick, Ireland.

10 ^dSchool of Earth and Environment, University of Leeds, Leeds LS2 9JT, United Kingdom.

11 ^eDesign and Manufacturing Technology, University of Limerick, Castletroy, Co. Limerick,
12 Ireland.

13 ^fDepartment of Applied Biotechnology and Food Science, Faculty of Chemical Technology
14 and Biotechnology, Budapest University of Technology and Economics, Műegyetem rkp. 3,
15 1111 Budapest, Hungary

16

17

18 *Corresponding Author. Tel: +353 91 495364; fax: +353 91 494507. E-mail address:

19 mark.healy@nuigalway.ie

20

21 **Highlights**

- 22 • Separate size fractions of bauxite residue were treated with gypsum and seawater.
- 23 • Alkalinity was reduced following treatment with the gypsum and seawater.
- 24 • The effect on composition and P adsorption of the treated samples were examined.
- 25 • Gypsum was found to be the most successful in enhancing the P adsorption capacity.

26

27 **Abstract**

28 Bauxite residue (red mud), the by-product produced in the alumina industry, is being
29 produced at an estimated global rate of approximately 150Mt per annum. Due to its highly
30 alkaline nature, many refineries use neutralisation techniques such as mud farming
31 (atmospheric carbonation), direct carbonation using carbon dioxide or reactions with
32 seawater, to treat the bauxite residue and reduce its alkalinity prior to disposal in the BRDA
33 (bauxite residue disposal area). Applying a treatment can render the bauxite residue non-
34 hazardous and may also prepare the bauxite residue for reuse, particularly as an adsorbent. In
35 this study, gypsum and seawater treatments were applied to the various bauxite residue
36 samples obtained and the effects on its mineral, elemental and physiochemical properties
37 were examined, as well as the effect on its phosphorus (P) adsorption capacity. It was found
38 that in addition to reducing the alkalinity of all bauxite residue samples used, the P adsorption
39 capacity was also enhanced following amendment with seawater or gypsum, particularly with
40 gypsum. A positive correlation was detected between P adsorption and both Ca and CaO. A
41 negative correlation was detected between the P adsorption and pH of the media. Fitting the
42 data obtained from a batch adsorption experiment to the Langmuir adsorption isotherm, the
43 maximum adsorption capacity was estimated to range from 0.345 to 2.73 mg P per g bauxite
44 residue, highlighting the re-use potential for bauxite residue as an adsorbent for P.

45

46 **Keywords:** bauxite residue; adsorption; bauxite residue filter; aqueous solution; phosphate
47 removal

48

49

50

51

52 **1. Introduction**

53 During the extraction of alumina from bauxite ore using the Bayer process, a by-product
54 called bauxite residue (red mud) (Kirwan et al., 2013; Liu et al., 2014) is produced. The
55 global inventory for bauxite residue is approximately 3 billion tonnes, with an estimated
56 annual production rate of 150 million tonnes (Evans, 2016; Mayes et al., 2016). Bauxite
57 residue is highly alkaline ($\text{pH} > 10$) (Goloran et al., 2013), with a high salinity and sodicity
58 (Gräfe et al., 2009). Current best practice within this industry includes careful planning and
59 management of highly engineered bauxite residue disposal areas (BRDAs), avoiding
60 contamination of the surrounding environment (Prajapati et al., 2016). In addition, some
61 refineries use neutralisation techniques for the bauxite residue before disposal into the
62 BRDAs (Klauber et al., 2011; IAI, 2015; Evans 2016). These techniques include (1) direct
63 carbonation, whereby the residue slurry is treated with either carbon dioxide, sulfur dioxide
64 gas, or undergoes intensive mud farming using amphirollers (atmospheric carbonation)
65 (Cooling, 2007; Fois et al. 2007; Dilmore et al., 2009; Evans, 2016) (2) addition of spent
66 acids and/or gypsum ($\text{CaSO}_4 \cdot 2\text{H}_2\text{O}$) (Kirwan et al., 2013), or (3) reaction of residues with
67 seawater (Hanahan et al., 2004; Palmer and Frost, 2009; Couperthwaite et al., 2014).

68

69 Bauxite residues typically comprise very fine particles, ranging from $0.01 \mu\text{m}$ to $200 \mu\text{m}$
70 (Pradhan et al., 1996). Depending on the type of bauxite ore used, in some refineries the
71 bauxite residue undergoes a separation technique during processing (Evans, 2016), which
72 allows it to be separated into two main fractions: a fine fraction with a particle size $< 100 \mu\text{m}$
73 and a coarse fraction with a particle size $> 150 \mu\text{m}$ (Eastham et al., 2006; Jones et al., 2012).
74 The coarse fraction mainly consists of quartz (SiO_2), whereas the fine fraction is dominated
75 by iron (Fe) oxides (Snars and Gilkes, 2009). The ratio of the fine to coarse fraction produced
76 is dependent on the bauxite ore used and the Bayer process employed (Li, 2001). Refineries

77 which carry out the separation technique, have found use for the coarse fraction to create
78 roadways to the BRDA and/or storage embankments (Evans, 2016). However, finding
79 appropriate options for the re-use of the fine fraction bauxite residue remains elusive (Power
80 et al., 2011; IAI, 2015).

81

82 Fine fraction bauxite residue comprises Fe oxides (20-45%) and aluminium (Al) oxides (10-
83 22%) (IAI 2015), which make it suitable as a medium to adsorb phosphorus (P). The
84 European Commission (EC) has identified waste management as an important aspect of the
85 “circular economy” (EC, 2015), so in recent years, emphasis has been placed on investigating
86 alternative methods of P recovery from wastewater (Grace et al., 2015, 2016). A move from
87 the more conventional methods of P recovery such as biological removal and chemical
88 precipitation (Wang et al., 2008), to the use of low-cost adsorbents from industrial solid
89 wastes, such as bauxite residue, have been examined. In comparison to standard P removal
90 by sand, bauxite residue has a high P retention capacity (Vohla et al., 2007). However, its P
91 removal potential is enhanced following treatment by heat, acid or gypsum (Table 1). Of the
92 methods employed, acid and heat treatment have proved most successful in increasing the P
93 adsorption capacity of the bauxite residue, with maximum adsorption capacities of up to 203
94 mg P g⁻¹ bauxite being achieved (Liu et al., 2007) compared to untreated residue (0.20 mg P
95 g⁻¹; Grace et al., 2015) (Table 1). However, whilst acid and heat treatments have proven to be
96 very successful in increasing the adsorption capacity of bauxite residue, they are expensive,
97 energy consuming (using high temperatures up to 700°C) (Xue et al., 2016), and, without
98 further treatment, do not allow for the easy reuse of the bauxite residue (e.g. as a possible
99 media for plant growth) (Xue et al., 2016).

100

101 Treatments such as seawater or gypsum provide relatively inexpensive, alternative
102 treatments, which may not only enhance the P adsorption capacity of the bauxite residue
103 media, but may also help to improve its physicochemical characteristics. Seawater treatment
104 improves bauxite's physical structure, due to the addition of magnesium (Mg) and calcium
105 (Ca) which behave as flocculating agents, allowing many of the fine particles in bauxite
106 residue to form more stable aggregates (Jones and Haynes, 2011), and a partial decrease in
107 sodium (Na) due to ion exchange with Mg, Ca and potassium (K) (Hanahan et al., 2004).
108 Seawater-treated bauxite residues also allow adsorbed P to become bio-available, unlike the
109 metal cations which are unavailable, highlighting the P and metal retention capabilities
110 (Fergusson, 2009). Revegetation of bauxite residue using gypsum has also improved plant
111 growth by reducing its alkalinity and salinity, and improving the structure of the residue
112 (Courtney et al., 2009; Courtney and Kirwan, 2012). In addition to this, modern alumina
113 refineries are often located close to deep water ports, to allow for the bulk shipment of
114 incoming bauxite (sometimes from multiple sources) to the refinery and/or for bulk shipment
115 of alumina to aluminium smelters situated elsewhere. Therefore, there is ample scope for the
116 increasing use of seawater neutralization technology for pre-treatment of residues in
117 refineries not already employing treatments previously mentioned, prior to their deposition in
118 the BRDA.

119
120 To the best of the authors' knowledge, no study has previously compared the use of raw
121 seawater or gypsum treatments on the separate fractions of bauxite residue as a method of
122 neutralisation and preparation for the re-use of bauxite residue in its separated and
123 unseparated fractions as low-cost adsorbents and a potential source of P. The objectives of
124 this study were to (1) characterise bauxite residue from two different sources, before and after
125 treatment with seawater and gypsum, and to investigate their potential to release trace

126 elements (2) investigate the effect of the treated bauxite residue on P adsorption (3) assess the
127 impact of particle size, mineral and elemental (particularly Ca and Mg) composition of the
128 bauxite residue on the adsorption of P.

129

130 **2. Materials and Methods**

131

132 2.1 Sample preparation

133 A one kilogram, sample of fresh bauxite residue was obtained from Alteo Gardanne
134 [Gardanne, France (43°27'9"N, 5°27'41" E)], who operate a co-disposal method for fine and
135 coarse fractions of bauxite. This sample will be referred to hereafter as UFR. One kilogram
136 of mud-farmed bauxite residue samples (treated by atmospheric carbonation and therefore
137 non-hazardous), were also obtained from Rusal Aughinish Alumina [Limerick, Ireland
138 (52°37'06"N, 9°04'19"W)], who separate the fine (particle sizes <100 µm) and coarse
139 (particle sizes >150 µm) fraction of bauxite residue before disposal (IAI 2015) in a ratio of
140 9:1 (fine: coarse). The fine and coarse fractions will be referred to hereafter as UF (untreated
141 fine) and UC (untreated coarse).

142

143 Before any analysis or experiments were conducted, all bauxite residue samples were dried at
144 105°C for 24 hr. Once dry, the samples were pulverised using a mortar and pestle and sieved
145 to a particle size <2 mm. 0.3 kg of each sample were then treated with either seawater (S) or
146 laboratory-grade gypsum (G) (Lennox, Ireland), so two treatments were applied to each
147 source of bauxite residue. S or G, placed after the above abbreviations, indicates the
148 treatment applied. Gypsum was applied to the 0.3 kg bauxite residue samples at a ratio of 8%
149 (w/w) (Lopez et al., 1998) and leached for 72 hr in accordance with standard methods (BSI,
150 2002). Seawater amendment involved mixing with 0.3 kg bauxite at a ratio of 5:1 (v/w)

151 (after Johnston et al., 2010), for 1 hr, followed by a 12 hr settlement period overnight. The
152 bauxite residue and seawater mixture was then filtered through a 0.45 μm membrane using a
153 vacuum pump. The treated bauxite residue samples were then oven dried for 24 hr,
154 pulverised with a mortar and pestle, and sieved to <2 mm in size.

155

156 2.2 Characterisation Study

157 Untreated and treated bauxite samples were characterised ($n=3$) for their physical, chemical,
158 elemental and mineralogical properties. Soil pH and electrical conductivity (EC) were
159 measured in an aqueous extract, using 5 g of bauxite residue sample in a 1:5 ratio (solid:
160 liquid) (Courtney and Harrington, 2010). The bulk density (ρ_b) was determined after Blake
161 (1965) and the particle density (ρ_p) after Blake and Hartge (1986) using 10 g of bauxite
162 residue samples. Total pore space (S_t) was calculated using the values obtained for the bulk
163 and particle densities (Danielson and Sutherland, 1986). The effective particle size analysis
164 (PSA) was determined on particle sizes <53 μm using optical laser diffraction on the Malvern
165 Zetasizer 3000HS® (Malvern, United Kingdom) with online autotitrator and a Horiba LA-
166 920, and reported at specific cumulative % (10, 50 and 90%). Mineralogical detection was
167 carried out using X-ray diffraction (XRD) on 1 g samples using a Philips X'Pert PRO MPD®
168 (California, USA), whilst surface morphology and elemental detection were carried out using
169 scanning electron microscopy (SEM) and energy-dispersive X-ray spectroscopy (EDS) on a
170 Hitachi SU-70 (Berkshire, UK), using approximately 1 g samples. Quantification of the
171 elemental content was carried out on 1 g samples by Brookside Laboratories (OH, USA) after
172 digestion (EPA, 1996) using Inductively Coupled Plasma Atomic Emission Spectroscopy
173 (ICP-AES) and elemental composition quantified using X-ray fluorescence (XRF).
174 Measurement of the point of zero charge (PZCpH) was after Vakros et al. (2002) using 1 g
175 samples, and cation exchange capacity (CEC) was determined using the K saturation

176 technique (Thomas, 1982), using 5 g samples. Brunauer-Emmett-Teller specific surface area
177 (SSA) and pore volume analysis were conducted on 1 g samples, which were degassed at
178 120°C for 3 hr prior to analysis carried out by Glantreo Laboratories (Cork, Ireland).

179

180 2.3 Phosphorus Adsorption Batch Study

181 The P adsorption capacity of nine bauxite samples (untreated and gypsum/seawater treated
182 samples) were examined in a bench-scale experiment. To conduct a P adsorption isotherm
183 test, ortho-phosphorus ($\text{PO}_4^{3-}\text{-P}$) solutions were made up to known concentrations using
184 potassium dihydrogen phosphate (K_2HPO_4) in distilled water. One gram of each of the sieved
185 media was placed into a series of 50 ml-capacity containers and was overlain with 25 ml of
186 the solutions. Each sample was then shaken in a reciprocal shaker at 250 rpm for 24 hr. At t
187 = 24 hr, the supernatant water from each sample container was filtered using $0.45\mu\text{m}$ filters
188 and analysed immediately using a nutrient analyser (Konelab 20, Thermo Clinical
189 Labsystems, Finland). The data obtained from the P adsorption batch studies were modelled
190 using the Langmuir adsorption isotherm (McBride, 2000), which assumes monolayer
191 adsorption on adsorption sites and allows for the estimation of the maximum P adsorption
192 capacity (q_{max}) of the media:

193

$$194 \quad q_i = q_{\text{max}} \left(\frac{k_a C_e}{1 + k_a C_e} \right) \quad (1)$$

195

196 where q_i is the quantity of the contaminant adsorbed per gram of media (g g^{-1}), C_e is the
197 equilibrium contaminant concentration in the water (g m^{-3}), k_a is a measure of the affinity of
198 the contaminant for the media ($\text{m}^3 \text{g}^{-1}$), and q_{max} is the maximum amount of the contaminant
199 that can be adsorbed onto the media (g g^{-1}).

200

201 2.3.1. Mobilization of Metals

202 To determine whether the residue media released trace elements, 25 mL of water was mixed
203 with 1 g of media for 24 hr and the supernatant was analysed by ICP-MS. The elements
204 selected for detection were Al, arsenic (As), barium (Ba), beryllium (Be), boron (B),
205 cadmium (Cd), Ca, chromium (Cr), copper (Cu), Fe, gallium (Ga), K, lead (Pb), Mg,
206 manganese (Mn), mercury (Hg), molybdenum (Mo), Na, nickel (Ni), P, selenium (Se), silicon
207 (Si), titanium (Ti), vanadium (V), and zinc (Zn).

208

209 2.4 Statistical analysis

210 Linear regression analysis was utilised to examine the extent of correlation between the
211 individual characteristic parameters of the bauxite residue samples and bauxite adsorption,
212 using Minitab. A Pearson correlation coefficient and a correlation p-value were determined to
213 quantify correlation. The p-value represents the probability that the correlation between the
214 bauxite residue characteristic in question and the response variable (adsorption) is zero i.e.
215 the probability that there is no relationship between the two.

216

217 **3. Results and Discussion**

218

219 3.1 Characterisation of bauxite residue

220

221 3.1.1 Effect of treatments on elemental and mineralogical composition

222 The mineral and total elemental composition of the three untreated bauxite residues [UF
223 (untreated fine fraction), UC (untreated coarse fraction), and UFR (untreated co-disposed)]
224 are shown in Tables 2 and 3. Bauxite residues are typically high in Fe and Al oxides (Liu et

225 al., 2007), which was found to be the case in this study. The mineralogical composition
226 present for all untreated samples was dominated by Fe_2O_3 , Al_2O_3 , SiO_2 and CaO . A decrease
227 in Al_2O_3 was noted following treatment with the gypsum and the seawater in all samples,
228 with an increase in CaO content noted in samples treated with gypsum.

229

230 XRD analysis showed that the main crystalline phases present in UF were haematite (Fe_2O_3),
231 goethite ($\text{FeO}(\text{OH})$), perovskite (CaTiO_3), boehmite ($\text{AlO}(\text{OH})$), rutile (TiO_2), gibbsite
232 $\text{Al}(\text{OH})_3$ and sodalite $\text{Na}_8(\text{Al}_6\text{Si}_6\text{O}_{24})\text{Cl}_2$ (Figure S1 in the Supplementary Material).

233 Similarly, the main minerals in UFR were haematite (Fe_2O_3), goethite ($\text{FeO}(\text{OH})$), boehmite
234 ($\text{AlO}(\text{OH})$), rutile (TiO_2), gibbsite $\text{Al}(\text{OH})_3$ and sodalite $\text{Na}_8(\text{Al}_6\text{Si}_6\text{O}_{24})\text{Cl}_2$ (Figure S2).

235 Boehmite ($\text{AlO}(\text{OH})$), rutile (TiO_2), gibbsite $\text{Al}(\text{OH})_3$ haematite (Fe_2O_3) were the
236 predominant minerals present in UC (Figure S3). Following treatment with seawater and
237 gypsum, a change in mineral phase in UFG, UFS, UFRS and UFRG occurred (Figure S4, S5,
238 S6, S7). After treatment with gypsum, a higher presence of the calcium carbonate, calcite
239 (CaCO_3), was detected in UFRG and UCG (Figure S7 and S8), and post seawater treatment,
240 small peaks representing brucite ($\text{Mg}(\text{OH})_2$) were detected in UFS and UCS (S5 and S9).

241

242 These findings are similar to previous studies that examined various neutralization techniques
243 for bauxite residue (Gräfe et al., 2009). When seawater is added to bauxite residue, a reaction
244 occurs where the hydroxide, carbonate and aluminate ions are eliminated due to a reaction
245 involving Mg^{2+} and Ca^{2+} (from the seawater) (Gräfe et al., 2009; Palmer and Frost, 2009).

246 This results in the formation of alkaline solids such as the calcium carbonates, calcite and
247 brucite, which cause a buffering effect, evidenced in a shift of pH to between 8 and 9 (Power
248 et al., 2011). The addition of gypsum (CaSO_4) results in a drop in the pH (approximately 8.6)
249 due to the precipitation of excess hydroxides (OH^-), aluminium hydroxides ($\text{Al}(\text{OH})_4^-$),

250 carbonates (CO_3^{2-}) to form calcium hydroxide/lime ($\text{Ca}(\text{OH})$), tri-calcium aluminate (TCA),
251 hydrocalumite and calcium carbonate (CaCO_3), which behave as buffers and maintain pH
252 (Gräfe et al., 2009). The addition of Ca also flocculates and helps with the formation of more
253 stable aggregates (Jones and Haynes, 2011).

254

255 An analysis of water samples (Table S1) to examine mobilisation of metals showed that As,
256 Al and Cr were present in the leachate from the UFR sample, but decreased following
257 gypsum and seawater treatments. Arsenic, Fe and Al were mobilised from the UF sample,
258 but these concentrations were reduced following treatment with gypsum and seawater.

259 Aluminium was mobilised from the UC. The reduction in Fe and Al following treatment
260 with either gypsum or seawater is in line with previous studies, which have shown that water
261 soluble Fe and Al decrease following gypsum application (Courtney and Timpson, 2005).

262 Overall, Al still remained above the maximum allowable concentration (MAC) of 0.2 mg L^{-1}
263 ($200 \mu\text{g L}^{-1}$) (EPA, 2014) for Al for drinking water. Sodium was still at a high level
264 following gypsum and seawater treatments, ranging from 139.3 ± 3.2 to $153 \pm 24.8 \text{ mg L}^{-1}$ and
265 241.3 ± 26 to $388.7 \pm 18.6 \text{ mg L}^{-1}$, respectively. The MAC for Na in drinking water is 200 mg
266 L^{-1} (EPA, 2014).

267

268 3.1.2 Effect of treatments on physicochemical properties

269 The untreated bauxite residues had high pH (10.8 ± 0.12 to 11.9 ± 0.06) and EC (704 ± 90.8 to
270 $1184 \pm 48.8 \mu\text{S cm}^{-1}$) (Table 4). Following treatment with gypsum and seawater, pH decreased
271 and EC increased. Changes for pH after treatment with either seawater or gypsum are due to
272 precipitation of calcium carbonates such calcite, brucite and aragonite, which behave as
273 buffers and maintain a reduced pH (Menziés et al., 2004), while the increase in EC is
274 attributed to the introduction of excess Na^+ and Ca^{2+} (Gräfe et al., 2009). The pH of bauxite

275 residue is normally within the range of 11 to 13 (Newson et al., 2006), but varies due to the
276 type of bauxite ore, Bayer process, and neutralisation techniques used in the refinery. Both
277 seawater (Menzies et al., 2004; Johnston et al., 2010) and gypsum applications (Jones and
278 Haynes, 2011; Courtney and Kirwan, 2012; Lehoux et al., 2013) are recognised methods of
279 reducing the alkalinity of bauxite residues.

280

281 No change was observed in the particle size or particle size density following the addition of
282 the gypsum and seawater treatments to the various bauxite residue samples (Table 4).

283 Similarly, the addition of gypsum or seawater did not have any impact on bulk density (Table
284 4).

285

286 The surface morphology of bauxite residues typically comprises 30% amorphous and 70%
287 crystalline phase (Gräfe et al., 2009). However, in this study SEM imaging suggests that the
288 bauxite residue samples were not present in strong crystalline form (Figure 1), in particular
289 for samples UF and UFR, as no distinctive crystalline structure to the bauxite residue samples
290 was observed. Liu et al. (2007) examined the effect of age on stored bauxite residue, and
291 found that fresh bauxite residue particles are present in poorly formed crystallised or
292 amorphous form in comparison to older bauxite residue (10 years), which has a stronger
293 crystalline formation, indicating that crystallisation occurs in some of the minerals over time.
294 As the bauxite residue used in this study was fresh, this would explain why there was not a
295 strong distinction between amorphous or crystalline forms, similar to the findings of Liu et al.
296 (2007). The composition of fine particles and larger particles in the coarse fraction (UC) were
297 noticeable from the SEM (Figure 1).

298

299 Improved aggregate formation was noticeable in the gypsum and seawater-treated bauxite
300 residues (Figure 1), due to the addition of Ca^{2+} , which results in flocculation (Zhu et al.,
301 2016). Changes in the surface morphology were also evident in the gypsum and seawater-
302 treated residues in comparison to the untreated residues, which appeared to have a much
303 smoother surface (Figure 1). This change in surface morphology following the treatments
304 was attributed to the changes in mineral phase (Huang et al., 2008).

305

306 3.2 Phosphorus Adsorption Study

307

308 3.2.1 Effect of seawater and gypsum treatment on P adsorption

309 All nine bauxite residue samples in this study were successful in removing P from aqueous
310 solution (Table 5). Bauxite residue has been shown in numerous P adsorption studies to have
311 a high P retention capacity, particularly following treatment or modification (Ye et al., 2014;
312 Grace et al., 2015). In this study, gypsum or seawater treatment had a positive impact on P
313 removal, with the gypsum-treated bauxite residue performing best (Table 5).

314

315 Following seawater treatment, the P adsorption capacity of the bauxite residues increased to
316 q_{max} values of 0.48, 0.66 and 1.92 mg P g^{-1} media for UFS, UCS and UFRS, respectively. In
317 previous studies, following treatment with seawater, bauxite residue had a higher adsorption
318 capacity for P. Akhurst et al. (2006) reported a maximum adsorption of 6.5 mg P g^{-1} when
319 using a bauxite residue treated with brine (BauxsolTM). This relatively high adsorption may
320 be attributed to the higher concentrations of Ca^{2+} and Mg^{2+} in the brines (or products such as
321 BauxsolTM, developed by BaseconTM), in comparison to raw seawater (0.41, 1.29 and 10.77 g
322 kg^{-1} of Ca^{2+} , Na and Mg^{2+} , respectively) used in this study (Gräfe et al., 2009). The gypsum-
323 treated bauxite residues had the highest q_{max} values – 2.46, 1.39 and 2.73 mg P g^{-1} media for

324 UFG, UCG and UFRG, respectively. However, these values were lower than a P adsorption
325 study carried out by Lopez et al. (1998), who used the same application rate of gypsum to the
326 bauxite residue samples and reported a q_{\max} of 7.03 mg P g⁻¹. The lower rate observed in the
327 current study may be attributed to the 72 hr leaching process that the gypsum-treated bauxite
328 residue underwent before use in the adsorption study, which may have allowed for further
329 exchange and removal of Ca²⁺ following the leaching process.

330

331 Overall, the bauxite residue in the current study had a higher P adsorbency than in other
332 studies for zeolite (0.01 mg P g⁻¹, Grace et al., 2015) and granular ceramics (0.9 mg g⁻¹; Chen
333 et al., 2012), but lower than fly ash, granular blast furnace slag and pyritic fill (6.48, 3.61 and
334 0.88 mg P g⁻¹, respectively; Grace et al., 2015), crushed concrete (19.6 mg P g⁻¹; Egemose et
335 al., 2012), untreated biochar (32 mg P g⁻¹; Wang et al., 2015), and NaOH-modified coconut
336 shell powder (200 mg P g⁻¹; de Lima et al., 2012).

337

338 3.2.2 Factors affecting P adsorption

339 The adsorption of P onto media is influenced by many factors which include particle size, pH,
340 component and surface characteristics (Wang et al., 2016). Numerous studies have
341 investigated the effect of parameters such as kinetics of P adsorption (Akhurst et al., 2006;
342 Liu et al., 2007; Ye et al., 2014; Grace et al., 2015), ionic solution (Akhurst et al., 2006), pH
343 (Liu et al., 2007; Huang et al., 2008; Grace et al., 2015) on the adsorption of P from aqueous
344 solution. While all bauxite residue samples in this study did remove P from aqueous solution,
345 it is clear that the application of treatments, such as gypsum or seawater, has an effect on the
346 adsorption capability, and that the rate of adsorption will vary as a result of the source of
347 bauxite residue and treatments used (Wang et al., 2008).

348

349 The parameters which showed a statistically significant positive correlation of medium
350 strength with P adsorption in this study were Ca (correlation coefficient = 0.47, $p = 0.01$,
351 Degrees of Freedom (DoF) = 25) and CaO (correlation coefficient = 0.39, $p = 0.04$, DoF =
352 25). A statistically significant negative correlation of medium strength was also detected
353 between pH and P adsorption (correlation coefficient = - 0.38, $p = 0.05$, DoF = 25). pH was
354 a contributing factor to the adsorption process with the amount of phosphate adsorbed
355 increasing with a decrease in pH in the media following treatments, UFRG>UFRS>UFR,
356 UFG>UFS>UF, UCG>UCS>UC. This was a similar finding to several studies carried out
357 (Li et al., 2006; Liu et al., 2007; Huang et al., 2008; Grace et al., 2015). The Ca ions also
358 influenced P adsorption. This is as a result of the high level of Ca^{2+} and Mg^{2+} present in the
359 bauxite residue, particularly after seawater and gypsum treatments, when the majority of
360 PO_4^{3-} is removed from solution due to the formation of magnesium phosphate ($\text{Mg}_3(\text{PO}_4)_2$)
361 and calcium phosphate ($\text{Ca}_3(\text{PO}_4)_2$) (Akhurst et al., 2006).

362

363 The pH at which net charges are neutral on the surface of the adsorbent - the point of zero
364 charge (PZC) - influences the rate of adsorption of P (Jacukowicz-Sobala et al., 2015). Where
365 the pH is higher than the PZCpH, the surface of the adsorbent media becomes more negative
366 (attracting more cations), as a result of the adsorption of OH^- from the surrounding solution
367 (Prajapati et al., 2016). The PZCpH ranged from 6.16 ± 0.21 to 6.96 ± 1.21 (Table 4) in the
368 three untreated samples. Following treatment with gypsum and seawater, there were notable
369 changes, but no statistical relevance was detected between the PZCpH and P adsorption in
370 this study. However, as bauxite residue is composed of numerous minerals, each with their
371 own individual PZCpH (which, as noted in the literature, can range from anywhere between
372 pH 2 to pH 9.8 (Gräfe et al., 2009)), this results in the bauxite residue being able to cater for a

373 wide range of pH (Gräfe et al., 2009) and also having the capability of removing both cations
374 and anions from solution.

375

376 The SSA analysis carried out on the bauxite residues show an increase in specific surface
377 area in all samples following treatment with either the gypsum or the seawater (Table 4).

378 There was also an increase in pore volume following the addition of either gypsum or
379 seawater (Table 4). This is attributed to the formation of precipitates formed in the

380 neutralisation process of both gypsum and seawater and the effect of the Ca acting as a

381 flocculant with the finer particles present. This increase in surface area also contributes to the

382 increase in P adsorption following treatments. Although particle size affects adsorption onto

383 media, due to the availability of sites for P uptake, no significant correlation was observed in

384 the current study.

385

386 3.3 Implications of the findings of this study

387 The use of gypsum and seawater treatments on bauxite residue improved the overall P

388 adsorption capacity of the bauxite residue samples, but mixing the bauxite residue and

389 treatments with actual wastewater will be necessary to fully understand the total adsorption

390 behaviour of the bauxite residue. In addition to improving the P adsorption, alkalinity was

391 significantly reduced following both treatments; however, the EC was increased. This may

392 limit the growth of plants on the gypsum or seawater-treated bauxite residues; therefore, one

393 option may be to increase the rinsing period of the bauxite residue following treatment to

394 remove the excess Ca^{2+} and Na^+ ions in solution. Lowering the alkalinity, increasing the P,

395 Ca^{2+} and Mg^{2+} content and improving the physical structure, provide the possible re-use

396 option of using the treated bauxite residue as a growth media.

397

398 For a refinery, the cost of neutralisation techniques is an obvious consideration when
399 deciding which technique(s) to use. The use of seawater as a neutralisation technique would
400 be a cheap and feasible option for a refinery that is close to the sea. The establishment of a
401 pipeline (if not already in place) would be the dominant capital cost. The use of a Nano
402 filtration system to concentrate the Ca^{2+} , Mg^{2+} and Na^+ ions in the seawater (Couperthwaite et
403 al., 2014) could allow for the reduction in volume of seawater necessary for the neutralisation
404 process, but may add to the cost. Gypsum however may be a more expensive option,
405 requiring machinery such as amphirolls for the mixing and spreading of the gypsum.
406 However, depending on the refinery's location, waste gypsum from construction sites or
407 fossil fuel powered power stations may be used (Jones and Haynes, 2011).

408

409 **4. Conclusions**

410

411 This study examined the impact of gypsum and seawater treatments on the mineral, elemental
412 and physiochemical properties of bauxite residue. The untreated bauxite residues were high
413 in Fe and Al oxides and their mineralogical composition was dominated by Fe_2O_3 , Al_2O_3 ,
414 SiO_2 and CaO . Following treatment with gypsum and seawater, the pH decreased and EC
415 increased, but no change was observed in the particle size or density. The SSA and pore
416 volume of the bauxite increased following both treatments, which contributed to increased P
417 adsorbency. Although the P adsorbency measured in this study was not as high as measured
418 in other studies using different media, it still indicates that reuse in water or wastewater
419 treatment facilities may be an appropriate option for bauxite residue.

420

421 **Acknowledgements**

422 The authors would like to acknowledge the financial support from the Irish Environmental
423 Protection Agency (EPA) (2014-RE-MS-1) and the UK Natural Environment Research
424 Council (NE/L01405X/1). The authors would also like to thank Rusal Aughinish Alumina and
425 Alteo Gardanne, who provided the bauxite residue sand and mud samples.

426

427

428

429

430

431

432

433

434

435

436

437

438

439

440

441

442

443

444

445

446

447 **References**

448

449 Akhurst, D.J., Jones, G.B., Clark, M., McConchie, D., 2006. Phosphate removal from
450 aqueous solutions using neutralised bauxite refinery residues (Bauxsol™). *Environ. Chem.* 3,
451 65-74.

452

453 Blake, G.R., 1965. Bulk density, in: Black, C.A. (Ed), *Methods of soil analysis. Part 1.*
454 *Physical and mineralogical properties, including statistics of measurement and sampling.*
455 ASA, SSSA, Madison, WI, pp. 374 – 390.

456

457 Blake, G.R., Hartge, K.H., 1986. Particle density, in: Klute, A. (Ed), *Methods of Soil*
458 *Analysis: Part 1—Physical and Mineralogical Methods.* SSSA, ASA, Madison, WI, pp. 377 –
459 382.

460

461 British Standard Institution, 2002. 12457-2. Characterisation of waste. Leaching. Compliance
462 test for leaching of granular waste materials and sludges. One stage batch test at a liquid to
463 solid ratio of 10 l/kg for materials with particle size below 4 mm (without or with size
464 reduction).

465

466 Chen, N., Feng, C., Zhang, Z., Liu, R., Gao, Y., Li, M., Sugiura, N., 2012. Preparation and
467 characterization of lanthanum (III) loaded granular ceramic for phosphorus adsorption from
468 aqueous solution. *J. Taiwan Instit. Chem. Eng.* 43, 783-789.

469

470 Cooling, D.J., 2007. Improving the sustainability of residue management practices-Alcoa
471 World Alumina Australia. In: (A. Fouri and R.J. Jewell, Eds) *Paste and Thickened Tailings:*

472 A Guide, 316.
473 <http://citeseerx.ist.psu.edu/viewdoc/download?doi=10.1.1.629.1067&rep=rep1&type=pdf>.
474 (accessed 31.10.17).
475
476 Couperthwaite, S.J., Johnstone, D.W., Mullett, M.E., Taylor, K.J., Millar, G.J., 2014.
477 Minimization of bauxite residue neutralization products using nanofiltered seawater. *Ind.*
478 *Eng. Chem. Res.* 53, 3787-3794.
479
480 Courtney, R.G., Timpson, J.P., 2005. Reclamation of fine fraction bauxite processing residue
481 (red mud) amended with coarse fraction residue and gypsum. *Water Air Soil Poll.* 164(1-4),
482 91-102.
483
484 Courtney, R.G., Jordan, S.N., Harrington, T., 2009. Physico- chemical changes in bauxite
485 residue following application of spent mushroom compost and gypsum. *Land. Degrad. Dev.*
486 20, 572-581.
487
488 Courtney, R., Harrington, T., 2010. Assessment of plant-available phosphorus in a fine
489 textured sodic substrate. *Ecol. Eng.* 36, 542-547.
490
491 Courtney, R., Kirwan, L., 2012. Gypsum amendment of alkaline bauxite residue—plant
492 available aluminium and implications for grassland restoration. *Ecol. Eng.* 42, 279-282.
493
494 Danielson, R.E., Sutherland, P.L., 1986. Porosity, in: Klute, A. (Ed), *Methods of soil*
495 *analysis. Part 1. Physical and Mineralogical Methods.* SSSA, ASA, Madison, WI, pp. 443-
496 461.

497

498 de Lima, A.C.A., Nascimento, R.F., de Sousa, F.F., Josue Filho, M., Oliveira, A.C., 2012.

499 Modified coconut shell fibers: a green and economical sorbent for the removal of anions from

500 aqueous solutions. *Chem. Eng. J.* 185, 274-284.

501

502 Dilmore, R.M., Howard, B.H., Soong, Y., Griffith, C., Hedges, S.W., DeGalbo, A.D.,

503 Morreale, B., Baltrus, J.P., Allen, D.E., Fu, J.K., 2009. Sequestration of CO₂ in mixtures of

504 caustic byproduct and saline waste water. *Environ. Eng. Sci.* 26, 1325-1333.

505

506 Eastham J, Morald T, Aylmore P., 2006. Effective nutrient sources for plant growth on

507 bauxite residue. *Water Air Soil Poll.* 176(1-4),5-19

508

509 Egemose, S., S nderup, M.J., Beinthin, M.V., Reitzel, K., Hoffmann, C.C., Flindt, M.R.,

510 2012. Crushed concrete as a phosphate binding material: a potential new management tool. *J.*

511 *Environ. Qual.* 41, 647-653.

512

513 EPA, 1996. EPA Method 3050B: Acid Digestion of Sediments, Sludges, and Soils.

514 www.epa.gov/sites/production/files/2015-06/documents/epa-3050b.pdf (accessed

515 30.10.2017).

516

517 EPA, 2014. Drinking Water Parameters Microbiological, Chemical and Indicator Parameters

518 in the 2014 Drinking Water Regulations.

519 www.epa.ie/pubs/advice/drinkingwater/2015_04_21_ParametersStandaloneDoc.pdf

520 (accessed 30.10.2017).

521

522 European Commission, 2015. COM 2015. 614 Communication from the commission to the
523 European Parliament, the Council, the European Economic and Social Committee and the
524 Committee of the regions - Closing the loop - An EU action plan for the circular economy.
525 Brussels.

526

527 Evans, K., 2016. The history, challenges, and new developments in the management and use
528 of bauxite residue. *J. Sustain. Metallurgy* 2, 316-331.

529

530 Fergusson, L., 2009. Commercialisation of environmental technologies derived from alumina
531 refinery residues: A ten-year case history of
532 Virotec. <http://citeseerx.ist.psu.edu/viewdoc/download?doi=10.1.1.458.2073&rep=rep1&typ>
533 [e=pdf](#) (accessed 8.12.17)

534

535 Fois, E., Lallai, A., Mura, G., 2007. Sulfur dioxide absorption in a bubbling reactor with
536 suspensions of Bayer red mud. *Ind. Eng. Chem. Res.* 46, 6770-6776.

537

538 Grace, M.A., Healy, M.G., Clifford, E., 2015. Use of industrial by-products and natural
539 media to adsorb nutrients, metals and organic carbon from drinking water. *Sci. Total.*
540 *Environ.* 518, 491-497.

541

542 Grace, M.A., Clifford, E., Healy, M.G., 2016. The potential for the use of waste products
543 from a variety of sectors in water treatment processes. *J. Clean. Prod.* 137, 788-802.

544

545 Goloran, J.B., Chen, C.R., Phillips, I.R., Xu, Z.H., Condrón, L.M., 2013. Selecting a nitrogen
546 availability index for understanding plant nutrient dynamics in rehabilitated bauxite-
547 processing residue sand. *Ecol. Eng.* 58, 228-237.

548

549 Gräfe, M., Power, G., Klauber, C., 2009. Review of bauxite residue alkalinity and associated
550 chemistry. CSIRO, Australia.

551 <http://enfo.agt.bme.hu/drupal/sites/default/files/vörösiszpa%20kémia%20és%20lúgosság.pdf>
552 (accessed 12.12.17)

553

554 Hanahan, C., McConchie, D., Pohl, H., Creelman, R., Clark, M., Stocksiek C., 2004.
555 Chemistry of seawater neutralization of bauxite refinery residues (red mud). *Environ. Eng.*
556 *Sci.* 21,125–138

557

558 Huang, W., Wang, S., Zhu, Z., Li, L., Yao, X., Rudolph, V., Haghseresht, F., 2008.
559 Phosphate removal from wastewater using red mud. *J. Hazard. Mater.* 158, 35-42.

560

561 IAI, 2015. Bauxite residue management: best practice. [http://www.world-](http://www.world-aluminium.org/media/filer_public/2015/10/15/bauxite_residue_management_-_best_practice_english_oct15edit.pdf)
562 [aluminium.org/media/filer_public/2015/10/15/bauxite_residue_management -](http://www.world-aluminium.org/media/filer_public/2015/10/15/bauxite_residue_management_-_best_practice_english_oct15edit.pdf)
563 [_best_practice_english_oct15edit.pdf](http://www.world-aluminium.org/media/filer_public/2015/10/15/bauxite_residue_management_-_best_practice_english_oct15edit.pdf). (accessed 14.10.2017).

564

565 Jacukowicz-Sobala, I., Ociński, D., Kociołek-Balawejder, E., 2015. Iron and aluminium
566 oxides containing industrial wastes as adsorbents of heavy metals: Application possibilities
567 and limitations. *Waste. Manage. Res.* 33, 612-629.

568

569 Johnston, M., Clark, M.W., McMahon, P., Ward, N., 2010. Alkalinity conversion of bauxite
570 refinery residues by neutralization. *J. Hazard. Mater.* 182, 710-715.
571

572 Jones, B.E., Haynes, R.J., 2011. Bauxite processing residue: a critical review of its formation,
573 properties, storage, and revegetation. *Crit. Rev. in Env. Sci. Tec* 41, 271-315.
574

575 Jones, B.E., Haynes, R.J., Phillips, I.R., 2012. Addition of an organic amendment and/or
576 residue mud to bauxite residue sand in order to improve its properties as a growth medium. *J.*
577 *Environ. Manage.* 95, 29-38.
578

579 Kirwan, L.J., Hartshorn, A., McMonagle, J.B., Fleming, L., Funnell, D., 2013. Chemistry of
580 bauxite residue neutralisation and aspects to implementation. *Int. J. Miner. Process.* 119, 40-
581 50.
582

583 Klauber, C., Gräfe, M., Power, G., 2011. Bauxite residue issues: II. options for residue
584 utilization. *Hydrometallurgy* 108, 11-32.
585

586 Lehoux, A.P., Lockwood, C.L., Mayes, W.M., Stewart, D.I., Mortimer, R.J., Gruiz, K.,
587 Burke, I.T., 2013. Gypsum addition to soils contaminated by red mud: implications for
588 aluminium, arsenic, molybdenum and vanadium solubility. *Environ. Geochem. Hlth* 35, 643-
589 656.
590

591 Li, L.Y., 2001. A study of iron mineral transformation to reduce red mud tailings. *Waste*
592 *Manage* 21, 525-534.
593

594 Li, Y., Liu, C., Luan, Z., Peng, X., Zhu, C., Chen, Z., Zhang, Z., Fan, J., Jia, Z., 2006.
595 Phosphate removal from aqueous solutions using raw and activated red mud and fly ash. J.
596 Hazard. Mater. 137, 374-383.
597
598 Liu, Y., Lin, C., Wu, Y., 2007. Characterization of red mud derived from a combined Bayer
599 Process and bauxite calcination method. J. Hazard. Mater. 146, 255-261.
600
601 Liu, W., Chen, X., Li, W., Yu, Y., Yan, K., 2014. Environmental assessment, management
602 and utilization of red mud in China. J. Clean. Prod. 84, 606-610.
603
604 Lopez, E., Soto, B., Arias, M., Nunez, A., Rubinos, D., Barral, M.T., 1998. Adsorbent
605 properties of red mud and its use for wastewater treatment. Water. Res. 32, 1314-1322.
606
607 Mayes, W.M., Burke, I.T., Gomes, H.I., Anton, A.D., Molnár, M., Feigl, V., Ujaczki, É.,
608 2016. Advances in understanding environmental risks of red mud after the Ajka spill,
609 Hungary. J. Sustain. Metallurgy. 2, 332-343.
610
611 Menzies, N.W., Fulton, I.M., Morrell, W.J., 2004. Seawater neutralization of alkaline bauxite
612 residue and implications for revegetation. J. Environ. Qual. 33, 1877-1884.
613
614 McBride, M.B., 2000. Chemisorption and precipitation reactions. Handbook of Soil Science.
615 CRC Press, Boca Raton, FL, B265-B302.
616
617 McConchie, D., Clark, M., Davies-McConchie, F., 2001. Processes and Compositions for
618 Water Treatment, Neauveau Technology Investments, Australian, p. 28.

619 Newson, T., Dyer, T., Adam, C., Sharp, S., 2006. Effect of structure on the geotechnical
620 properties of bauxite residue. *J. Geotech. Geoenviron.* 132, 143-151.
621

622 Palmer, S.J., Frost, R.L., 2009. Characterisation of bauxite and seawater neutralised bauxite
623 residue using XRD and vibrational spectroscopic techniques. *J. Mater. Sci.* 44, 55-63.
624

625 Power, G., Gräfe, M., Klauber, C., 2011. Bauxite residue issues: I. Current management,
626 disposal and storage practices. *Hydrometallurgy* 108, 33-45.
627

628 Pradhan, J., Das, S.N., Das, J., Rao, S.B., Thakur, R.S., 1996. Characterization of Indian red
629 muds and recovery of their metal values. Annual meeting and exhibition of the minerals,
630 metals and materials society, Anaheim, CA, 4 – 8 February 1996.
631

632 Prajapati, S.S., Najar, P.A., Tangde, V.M., 2016. Removal of Phosphate Using Red Mud: An
633 Environmentally Hazardous Waste By-Product of Alumina Industry. *Adv. Phy. Chemistry*,
634 2016.
635

636 Snars, K., Gilkes, R.J., 2009. Evaluation of bauxite residues (red muds) of different origins
637 for environmental applications. *Appl. Clay. Sci.* 46, 13-20.
638

639 Thomas, G.W., 1982. Exchangeable cations. *Methods of soil analysis. Part 2. Chemical and*
640 *microbiological properties, (methodsofsoilan2),* 159-165.
641

642 Vakros, J., Kordulis, C., Lycourghiotis, A., 2002. Potentiometric mass titrations: a quick scan
643 for determining the point of zero charge. *Chem. Commun.* 17, 1980-1981.

644

645 Vohla, C., Alas, R., Nurk, K., Baatz, S., Mander, Ü., 2007. Dynamics of phosphorus,
646 nitrogen and carbon removal in a horizontal subsurface flow constructed wetland. *Sci. Tot.*
647 *Environ.* 380, 66-74.

648

649 Wang, S., Ang, H.M., Tadó, M.O., 2008. Novel applications of red mud as coagulant,
650 adsorbent and catalyst for environmentally benign processes. *Chemosphere* 72, 1621–1635

651

652 Wang, B., Lehmann, J., Hanley, K., Hestrin, R., Enders, A., 2015. Adsorption and desorption
653 of ammonium by maple wood biochar as a function of oxidation and pH. *Chemosphere* 138,
654 120-126.

655

656 Wang, Z., Shen, D., Shen, F., Li, T., 2016. Phosphate adsorption on lanthanum loaded
657 biochar. *Chemosphere* 150, 1-7.

658

659 Xue, S., Zhu, F., Kong, X., Wu, C., Huang, L., Huang, N., Hartley, W., 2016. A review of the
660 characterization and revegetation of bauxite residues (Red mud). *Environ. Sci. Poll. Res.* 23,
661 1120-1132.

662

663 Ye, J., Zhang, P., Hoffmann, E., Zeng, G., Tang, Y., Dresely, J., Liu, Y., 2014. Comparison
664 of response surface methodology and artificial neural network in optimization and prediction
665 of acid activation of Bauxsol for phosphorus adsorption. *Water Air Soil Poll.* 225(12), 2225.

666

667 Zhu, F., Li, Y., Xue, S., Hartley, W., Wu, H., 2016. Effects of iron-aluminium oxides and
668 organic carbon on aggregate stability of bauxite residues. *Environ. Sci. Pollut. Res.* 23, 9073-
669 9081.

670

671

672

673

674

675

676

677

678

679

680

681

682

683

684

685

686

687

688

689

690

691

692 **Table 1** Phosphorus (P) adsorption studies that have been carried out using bauxite residues, untreated
 693 and treated residues, and their recovery efficiencies.

	P recovery technique	Factors investigated	Type of water	Initial P concentration of the water	P recovered	Reference
Untreated bauxite residue	Batch adsorption experiment	Kinetics, pH and temperature	Synthetic water	5-100 mg P L ⁻¹	0.20 mg P g ⁻¹	Grace et al. 2015
Gypsum Treated	Batch adsorption experiment	Contact time (3, 6, 24, 48hr)	Synthetic water	20-400 mg P L ⁻¹	7.03 mg P g ⁻¹	Lopez et al. 1998
Brine treated bauxite residue (Bauxsol™*)	Batch adsorption experiment	pH, ionic strength, time	Synthetic water	0.5-2 mg P L ⁻¹	6.5-14.9 mg P g ⁻¹	Akhurst et al. 2006
Acid and brine treated bauxite residue (Bauxsol™*)	Batch adsorption experiment	Kinetics and isotherms	Synthetic water	200 mg P L ⁻¹	55.72 mg P g ⁻¹	Ye et al. 2014
Heat treated bauxite residue	Batch adsorption experiment	Time, pH and initial concentration	Synthetic water	155 mg P L ⁻¹	155.2 mg P g ⁻¹	Liu et al. 2007
Acid and heat treated bauxite residue	Batch adsorption experiment	Time, pH and initial concentration	Synthetic water	155 mg P L ⁻¹	202.9 mg P g ⁻¹	Liu et al. 2007
Acid treated bauxite residue	Batch adsorption experiment	Acid type, pH	Synthetic water	1 mg P L ⁻¹	1.1 mg P g ⁻¹	Huang et al. 2008

694 *Bauxsol™ = neutralised bauxite residue produced using the Basecon™ procedure, which uses brines high in
 695 Ca²⁺ and Mg²⁺ (McConchie et al. 2001).

696
 697
 698
 699
 700
 701
 702
 703
 704

705
706

Table 2 Mineralogical composition of the bauxite residues, untreated and treated.

Parameter	Untreated Fine (UF)	Fine +gypsum (UFG)	Fine+ seawater (UFS)	Untreated Coarse (UC)	Coarse+ gypsum (UCG)	Coarse +seawater (UCS)	Untreated French (UFR)	French+ gypsum (UFRG)	French +seawater (UFRS)
Fe₂O₃ (%)	43.9±1.1	40.6±0.6	41.8±1.2	64.0±5.1	61.4±3.0	69.9±3.8	43.9±0.6	47.9±0.5	53.3±5.8
Al₂O₃ (%)	12.7±0.6	11.3±1.0	11.1±2.5	19.4±1.8	11.1±0.6	7.4±0.7	14.0±1.0	11.2±0.3	11.4±2.2
CaO (%)	5.9±0.2	8.2±0.5	4.4±0.3	1.1±0.2	7.6±0.4	1.2±0.1	5.6±0.1	7.7±0.3	3.2±0.5
MgO (%)	3.6±1.3	3.5±0.8	3.1±1.0	4.7±1.8	3.6±0.8	2.6±0.6	4.1±0.6	3.8±0.9	3.2±1.6
SiO₂ (%)	8.6±0.7	8.5±0.9	8.6±1.7	2.6±0.3	1.3±0.2	1.4±0.2	9.4±0.5	5.1±0.4	4.3±0.3
TiO₂ (%)	2.4±0.3	2.1±0.6	2.7±0.1	0.9±0.1	1.0±0.1	2.1±0.6	2.5±0.02	2.3±0.1	2.3±0.5
P₂O₅ (%)	0.6±0.04	0.4±0.02	0.4±0.1	0.3±0.02	0.2±0.02	0.2±0.06	0.5±0.01	0.5±0.02	0.5±0.01

Table 3 Elemental composition of the bauxite residues, untreated and treated.

Parameter	Untreated Fine (UF)	Fine +gypsum (UFG)	Fine+ seawater (UFS)	Untreated Coarse (UC)	Coarse+ gypsum (UCG)	Coarse +seawater (UCS)	Untreated French (UFR)	French+ gypsum (UFRG)	French +seawater (UFRS)
B (mg kg⁻¹)	470±8.81	425±29	448±13	615±13.3	622±29	722±32.1	566±18.9	539±25	483.8±31
Al (mg kg⁻¹)	72538±1390	81095±1219	80608±3090	45854±2769	48851±2336	45917±2080	67295±3343	65389±1326	64189±595
As (mg kg⁻¹)	21.9±1.73	9.7±0.4	<LOD ¹	<LOD ¹	<LOD ¹	<LOD ¹	8.1±0.2	9.75±0.6	6.51±0.43
Ba (mg kg⁻¹)	43.8±1.19	29.4±5	33.3±0.7	13.9±1.01	18.3±3.4	12.7±2.8	45.7±1.5	41.4±1.4	49.4±3.8
Cd (mg kg⁻¹)	8.033±0.16	7.02±0.3	7.33±0.19	10.7±0.18	10.8±0.5	11.8±0.59	9.31±0.2	8.87±0.3	8.21±0.3
Cr (mg kg⁻¹)	1698±37.2	933±44	1170±12.9	880±3.8	817±13	803±21.3	1184±15.9	1090±9	1159±31.2
Fe (mg kg⁻¹)	338571±3057	289459±1859	298282±4937	434739±9980	460078±23043	471204±25753	353392±10003	328114±4498	332251±3435
Pb (mg kg⁻¹)	34.88±0.54	27.8±2.8	36.9±0.8	29.56±3.03	24.6±3	22.06±2.47	34.5±0.9	32.3±0.8	37.4±2.1
Mg (mg kg⁻¹)	122.28±4.96	163±37	1047±25.6	18.32±4.78	8.5±2.21	511.6±25.4	109±3.9	150±9	2203.8±134
Mn(mg kg⁻¹)	163±2.63	140±6.1	167±6.8	187±15.5	223±99	185±31.1	134±0.9	139±1.9	142.9±4.2
Ni (mg kg⁻¹)	18.6±0.89	<LOD ¹	2.25±0.2	3.54±0.27	3.15±0.5	4.18±0.22	1.1±0.1	1.24±0.2	1.23±0.3
K (mg kg⁻¹)	391±13.68	454±29	1108±41	255±38	195±23	556.99±67.38	399±13	359±11	1048±63.2
Si (mg kg⁻¹)	223.5±46.1	256±92	245.7±35	213±6.6	234±34	194.46±10.58	276±20	285±34	258.5±11.7
Na (mg kg⁻¹)	28347±553	38180±352	41864±2012	8804±666	5935±114	11101.55±1121.8	25514±317	23703±499	31974±1087
Ti (mg kg⁻¹)	1395±196	1309±100	1265±22	<LOD ¹	<LOD ¹	<LOD ¹	1382±38	1288±120	1233±46
V(mg kg⁻¹)	1050±21.6	781±29	777±8	786±23.6	731±20	731.04±23	1036±12	920±7	983±21
Zn (mg kg⁻¹)	50.7±0.71	40.6±1.2	42.6±1.3	86.7±1.7	82±5.4	84.68±4.2	55.8±0.5	55.6±1.17	57.3±0.9
Ga(mg kg⁻¹)	78.9±2.02	81.2±0.53	73.9±0.6	71.8±1.03	69.3±2.3	73.5±1.6	86.8±1.3	78.6±2	78.8±0.9
Ca(mg kg⁻¹)	46657±832	51641±485	17159±413	4152±490	12771±823	4089.42±588.32	15084±358	42703±2383	14820±926
P(mg kg⁻¹)	955±0.57	962±99	1018±15	1040±23	1011±59	1039.6±23	1298±26	1220±10	1320±53.8
Be(mg kg⁻¹)	<LOD ¹	<LOD ¹	<LOD ¹	<LOD ¹	<LOD ¹	<LOD ¹	<LOD ¹	<LOD ¹	<LOD ¹
Cu (mg kg⁻¹)	<LOD ¹	<LOD ¹	<LOD ¹	<LOD ¹	<LOD ¹	<LOD ¹	<LOD ¹	<LOD ¹	<LOD ¹
Hg (mg kg⁻¹)	<LOD ¹	<LOD ¹	<LOD ¹	<LOD ¹	<LOD ¹	<LOD ¹	<LOD ¹	<LOD ¹	<LOD ¹
Mo(mg kg⁻¹)	<LOD ¹	<LOD ¹	<LOD ¹	<LOD ¹	<LOD ¹	<LOD ¹	<LOD ¹	<LOD ¹	<LOD ¹
Se (mg kg⁻¹)	<LOD ¹	<LOD ¹	<LOD ¹	<LOD ¹	<LOD ¹	<LOD ¹	<LOD ¹	<LOD ¹	<LOD ¹

¹<LOD = below the limits of detection.

708
709

Table 4 Physical and chemical characterisation of the bauxite residues, untreated and treated.

Parameter	Untreated Fine (UF)	Fine +gypsum (UFG)	Fine+ seawater (UFS)	Untreated Coarse (UC)	Coarse+ gypsum (UCG)	Coarse +seawater (UCS)	Untreated French (UFR)	French+ gypsum (UFRG)	French +seawater (UFRS)
pH	10.8±0.12	8.7±0.04	9.02±0.07	11.4±0.29	6.79±0.08	7.95±0.16	11.9±0.06	9.17±0.02	9.49±0.01
EC ($\mu\text{S cm}^{-1}$)	704±90.8	1338±3.5	3080±17.3	856±1.53	909±2	916±1.53	1184±48.8	1219±7.21	5323±172
% Water	23.5±0.65	28.9±0.6	32.1±1.72	0.39±0.2	0.82±0.18	3.13±0.72	28±0.54	35.3±1.32	36.5±0.16
d_{10} (μm) ^a	0.6±0.09	1.37±0.23	1.26±0.06	1.27±0.47	1.11±0.23	1.66±0.83	1.3±0.04	1.49±0.06	1.08±0.74
d_{50} (μm) ^b	2.43±0.29	3.56±0.59	3.52±0.11	5.13±0.63	3.69±0.49	3.68±0.4	3.7±0.12	4.11±0.39	3.47±0.98
d_{90} (μm) ^c	6.02±0.86	7.12±1.98	7.69±1.97	12.04±1.27	9.51±0.25	7.0±0.13	10.11±2.37	9.81±2.68	7.17±3.25
Total Pore Space (%) ^d	50.03±2.25	50.73±9.04	50.03±1.75	9.63±6.46	10.82±1.09	7.65±5.26	61.77±1.16	53.6±1.95	53.87±0.78
Bulk Density (g cm^{-3}) ^e	1.5±0.02	1.5±0.01	1.49±0.01	2.53±0.01	2.48±0.03	2.55±0.01	1.31±0.03	1.32±0.03	1.31±0.02
Particle Size Density (g cm^{-3}) ^f	2.99±0.1	3.11±0.5	2.94±0.12	2.81±0.21	2.65±0.4	2.7±0.14	3.41±0.07	2.85±0.08	2.85±0.07
PZCpH ^g	6.96±1.21	3.43±0.73	6.28±0.98	6.89±0.09	3.11±0.12	6.39±0.51	6.16±0.21	6.32±0.51	4.43±0.09
CEC (K)(cmol kg^{-1}) ^h	63.3±2.56	64.1±3.41	60.1±2.96	N/A ^k	N/A ^k	N/A ^k	57.5±2.13	56.4±3.49	48.9±13.7
Total Pore Volume (cm^{-3}) ⁱ	0.03	0.03	0.03	0.02	0.02	0.03	0.03	0.04	0.03
BET SSA ($\text{m}^2 \text{g}^{-1}$) ^j	11.73	12.77	13.82	12.58	13.19	15.37	15.24	17.57	17.57

710
711
712
713
714
715
716
717
718
719
720

^a d_{10} (μm) = the size of particles at 10% of the total particle distribution, expressed in μm .

^b d_{50} (μm) = the median; the size of particles at 50% of the total particle distribution, expressed in μm .

^c d_{90} (μm) = the size of particles at 90% of the total particle distribution, expressed in μm .

^dTotal Pore Space = the total pore space which may be calculated from particle density and bulk density.

^eBulk density = the mass of soil per unit volume, expressed as g cm^{-3} .

^fParticle size density = the density of the solid particles, excluding pore spaces between them, expressed as g cm^{-3} .

^gPZCpH = the pH at which the point of zero charge is occurring.

^hCEC= the cation exchange capacity, expressed as cmol kg^{-1} .

ⁱBET SSA = specific surface area analysed using Brunauer-Emmett-Teller isotherm and expressed as $\text{m}^2 \text{g}^{-1}$.

^jTotal Pore Volume = measurement of total pore volume expressed as $\text{cm}^{-3} \text{g}^{-1}$.

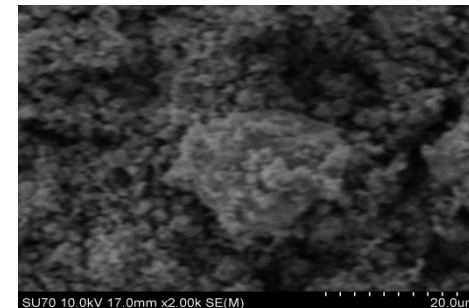
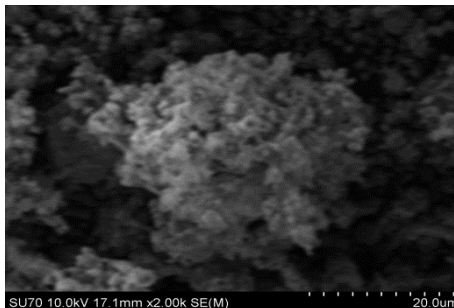
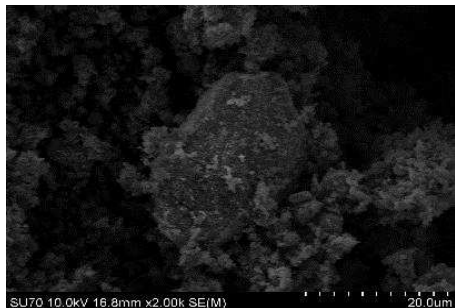
^kN/A =not available

721 **Table 5** Maximum adsorbency (mg P g^{-1} media) of P using each of the bauxite residue samples,
 722 untreated and treated (level of fit of the data, R^2 , to Langmuir isotherm is included in brackets).
 723

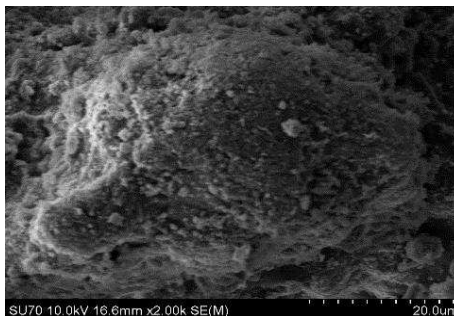
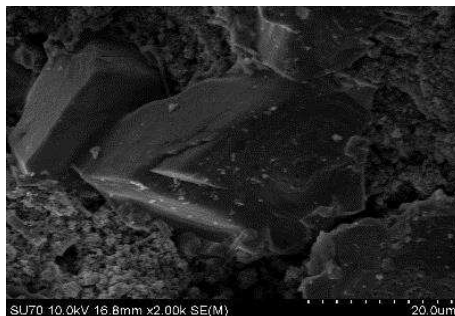
Media	Treatment method employed		
	Untreated	Gypsum	Seawater
	----- mg P g^{-1} media -----		
	-		
UFR	1 (0.99)	2.73 (0.99)	1.92 (0.99)
UF	0.38 (0.99)	2.46 (0.97)	0.48 (0.99)
UC	0.35(0.98)	1.39 (0.99)	0.66 (0.99)

724
 725
 726
 727
 728
 729
 730
 731
 732
 733
 734
 735
 736
 737
 738
 739

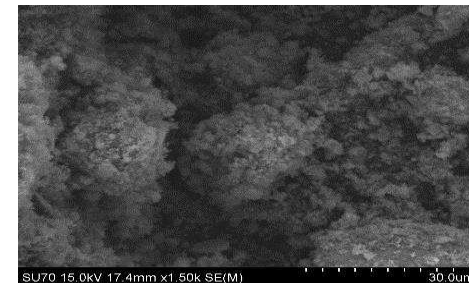
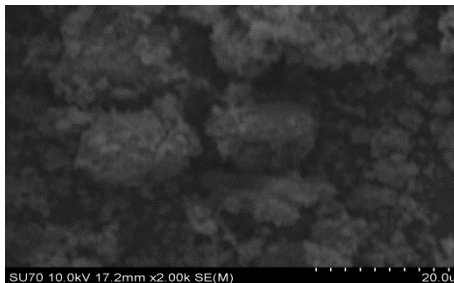
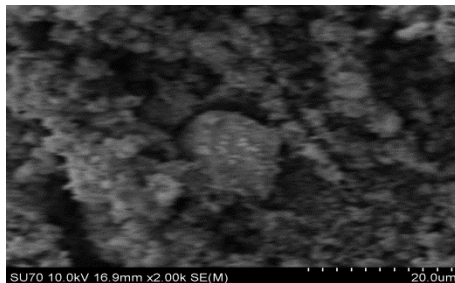
UF



UC



UFR



Untreated

Gypsum Treated

Seawater Treated

Figure 1. SEM (10kV; magnification x2,000; working distance 16.8mm) imaging for the three untreated bauxite residue pre and post treatment with either gypsum or seawater.

740